Journal of Plastic, Reconstructive & Aesthetic Surgery 97 (2024) 200–211

JPRAS
An International Journal of Surgical Reconstruction
www.JPRASurg.com

Tissue-engineered cellulose tubes for microvascular and lymphatic reconstruction: A translational and feasibility study

P.A. Will [a,b,c,*], F. Taqatqeh [a], F. Fricke [d], J.E. Berner [e,f], N. Lindenblatt [g], U. Kneser [b,c], C. Hirche [b,c,h]

[a] *Department of Plastic and Hand Surgery, Faculty of Medicine and University Hospital Carl Gustav Carus, TU Dresden, Dresden, Germany*
[b] *Department of Hand, Plastic, and Reconstructive Surgery, Microsurgery, Burn Centre BG Klinik Ludwigshafen, Ludwigshafen, Germany*
[c] *Plastic Surgery and Hand Surgery, University Heidelberg, Heidelberg, Germany*
[d] *Applied Tumor Biology, German Cancer Research Center, Heidelberg, Germany*
[e] *Kellogg College, University of Oxford, Oxford, United Kingdom*
[f] *Department of Plastic Surgery, The Newcastle upon Tyne Hospitals NHS Foundation Trust, Newcastle, United Kingdom*
[g] *Department of Plastic Surgery and Hand Surgery, Lymphatic Network of Excellence, University Hospital Zurich, Zurich, Switzerland*
[h] *Department of Plastic, Hand, and Reconstructive Microsurgery, Hand-Trauma and Replantation Center, BG Unfallklinik Frankfurt am Main, Affiliated Hospital of Goethe-University, Frankfurt am Main, Germany*

Received 14 October 2023; Accepted 24 May 2024

KEYWORDS
Tissue engineering;
Heterografts;
Microsurgery;
Lymphedema;
Anastomosis, surgical;
Cellulose

Summary *Background:* Lymphedema microsurgery is an emerging treatment modality, with dissimilar long-term outcomes. One of the main technical challenges in lymphatic microsurgery is the identification and availability of suitable donor vessels for anastomosis. Tissue engineering using biomaterials has demonstrated promise in addressing vessel quality issues in other fields, but its application in microsurgery is still limited.
Methods: Decellularized cellulose tubes were developed and bioengineered by decellularizing stems of *Taraxacum-Ruderalia*. The microscopic structure, mechanical properties, and residual DNA content of the cellulose tubes were evaluated. Human and murine skin fibroblasts and

Part of this work will be presented at the DAM conference in Bern on November 2023.

* Correspondence to: Plastic Surgery Department, University Hospital Carl Gustav Carus, TU Dresden, Fetscherstraße 74, Dresden 01307, Germany.
E-mail address: pwillmarks@yahoo.de (P.A. Will)

https://doi.org/10.1016/j.bjps.2024.05.043

dermal lymphatic endothelial cells were isolated and cultured for recellularization studies. Biocompatibility, proliferative capacity, and *ex-vivo* endothelialization of the cellulose tubes were assessed as potential interposition grafts. Finally, the engineered cellulose tubes were assessed as interposing xenografts for lymphovenous anastomoses (LVA) in an *ex-vivo* swine limb model.

Results: The decellularized cellulose tubes exhibited a suitable microscopic structure, mechanical properties, and low residual DNA content. The tubes showed adequate biocompatibility, supported cell proliferation, and facilitated spontaneous *ex-vivo* endothelialization of lymphatic endothelial cells. In the swine limb model, LVA using the engineered cellulose tubes was successfully performed.

Conclusion: This translational study presents the use of decellularized cellulose tubes as an adjunct for micro and supermicrosurgical reconstruction. The developed tubes demonstrated favorable structural, mechanical, and biocompatible properties, making them a potential candidate for improving long-term outcomes in lymphedema surgical treatment. The next translational step would be trialing the obtained tubes in a microsurgical in-vivo model.

Background

Following inadequate clinical improvement with conservative management in early-stage lymphedema, approximately 200 million patients with secondary lymphedema could potentially benefit from lymphatic microsurgery.[1,2] However, complex supermicrosurgical procedures such as lymphovenous anastomosis (LVA) or vascularized lymphatic tissue transfer (VLNT) are not readily accessible in most parts of the developing world.[3,4]

Recent meta-analyses proved the efficacy of prophylactic and therapeutic LVA. However, the outcomes are still heterogeneous, with great variability in surgical techniques and number of LVAs needed for achieving the best outcomes.[3-5] Accomplishing a patent supermicrosurgical anastomosis is technically challenging, particularly if the quality of donor and recipient vessels has been affected by chronic inflammation. Frequently, there is a gap between a suitable vein and a lymphatic vessel.[6,7] Most experts in lymphedema surgery have reported that segmental lymphosclerosis, the quality of the collector's wall, and the size mismatch between the lymph vessel and the venule are key technical challenges that limit anastomotic quality, patency, and feasibility.[8-13] Additionally, there is a risk that post-operative scarring may compress the microanastomosis leading to subsequent vessel occlusion.[14] Such technical challenges in the field of lymphatic supermicrosurgery and also in vascular microsurgical reconstruction could be overcome with tissue engineering.

Tissue engineering applications have already addressed poor quality vessels for hemodialysis vascular access and peripheral artery bypasses, using decellularized bovine carotid artery (Artegraft®) and bovine mesenteric vein (ProCol®) grafts.[15] *In-vitro* studies have demonstrated that decellularized vascular grafts allow the reseeding of endothelial cells, and that spontaneous reendothelialization occurs in these biological tubes.[16,17] Further studies on bioengineered tubes as vascular grafts have been developed, such as crosslinked collagen tubes tested as femoral artery interpositional grafts in murine models,[18] absorbable electrospun polylactide-copolactone,[19] or the creation of arteriovenous loops with decellularized placental vessels.[20] All these approaches are intriguing, yet the biggest limitation is that all of them involve conduits of animal origin. The exposed mammalian proteins present a substantial risk for thrombosis, immune rejection, and infection.[15] However, synthetic grafts might induce foreign body reaction, graft migration over time, and local chronic inflammation.[21]

In contrast to animal-based xenografts, polymers abundant in the exoskeletons of insects, shells, bacteria, and plants might be easily available and more suitable biomaterials for lymphatic tissue engineering. Chitin, chitosan, and cellulose are the most abundant organic macromolecules that are insoluble, chemically stable, sustainable, and inexpensive to produce.[22-24] Cellulose is known to be well tolerated by our immune system, and immune rejections or allergies have not been described.[25] Although chitin and chitosan nanofibrils are up to 3.0 Gpa strong and have rigid structures, cellulose fibrils are more bendable and therefore suitable as vascular biomaterials.[26,27] Chitin and cellulose share thermal insulation properties, antibacterial activity, mechanical stability, and the absence of cytotoxicity during biodegradation.[22-24] Moreover, chitin has proven hemostatic properties in whole, defibrinated, and heparinized blood,[28] and cellulose decreases intrinsic clotting ability and has therefore been used as the main biomaterial for hemodialysis membranes.[29] Cellulose grafts have recently been used in translational experiments such as bacterial cellulose tubes implemented to reconstruct the facial nerve of rats or in a further translational step such as the reconstruction of the tympanic membrane of patients suffering from tympanic membrane perforation.[30,31]

Although lymphatic tissue engineering is emerging as an adjuvant solution with the development of preconditioned hydrogel matrices and its selective *ex-vivo* vascularization, pragmatic translational solutions to aid microsurgical

reconstructions are still lacking.[32] The aim of the study was to bioengineer a decellularized cellulose-based tube, that is translationally suitable for vascular, microvascular, and lymphatic anastomoses.

Methods

Preparation of decellularized cellulose tube for cell culture and *ex-vivo* implantation

Fresh specimens of wild *Taraxacum-Ruderalia* were placed in phosphate-buffered saline (PBS)/0.25% Sodium dodecyl sulfate (SDS) (817034, Sigma, Germany) solution at room temperature (RT) for 24 h. Then, the stems were washed and incubated at 100 rpm and RT in a sterile solution of PBS/0.25% SDS for 7 days. Solutions were changed daily to enhance decellularization efficiency. After 8 detergent washing steps, the decellularized tubes were dried overnight under the laminar flow hood and UV light sterilization.

To determine the microscopic structure of the decellularized tubes, 0.5 mm tube samples were harvested, fixed in 4% paraformaldehyde, and embedded in paraffin. Tissue slices (5 μm) were cut from the sample blocks (CM3050S, Leica, Germany) and cellulose tissue was stained with fluorescent calcofluor white (CW)(18909, Sigma, Germany). For the analysis, confocal microscopy at 40X and 63X-magnification (TCS-SP8, Leica, Germany) was used.

To quantitatively evaluate the mechanical properties of the decellularized tubes, the hydrostatic conductivity at the average pressure of lymphatic collectors and density of lymph fluid were measured. The risk of kinking was determined by curving the conduit around a plastic template of predefined decreasing diameter ranging from 50 to 5 mm. The details of the kink resistance test are described elsewhere.[33] As comparative controls for the hydrostatic conductivity and kink resistance test, fresh arteries, veins, and lymphatic collectors were harvested from swine extremities and decellularized using the same method.

Isolation and cell culture of endothelial cells and fibroblasts

Dermal lymphatic endothelial cells (HDLEC, C-12210) were obtained from Promocell Heidelberg and cultured in endothelial cell growth medium (C-22120) according to the fabricant specifications. After reaching 90% confluency, the cells were resuspended in endothelial cell growth medium, seeded at a density of 5000 cells/cm^2 and cultured under sterile conditions at 37 °C in a 5% CO_2 incubator.

After obtaining ethical approval (Ärztekammer Rheinland-Pfalz Nr. 2020-15173 and Nr. G-206-15), full-thickness skin tissue samples were harvested during the induction of secondary lymphedema in the hind limbs of a murine model[34] and from patients undergoing reconstructive free flaps and thigh contouring procedures. The dermis was homogenized and incubated in collagenase I (9001121, Sigma, Germany) Hank's balanced salt solution (2 mg/ml) for 1-2 h at 37 °C. After inactivation of the enzyme and serial centrifugation, viable fibroblasts were seeded at a density of 5000 cells/cm^2 in T75 flasks and cultured in Dulbecco's Modified Eagle Medium/10% FCS at 37 °C in a 5% CO_2 atmosphere.

Quantification of DNA content in the tubes

The effectiveness of the decellularization protocol was tested by quantifying the remaining DNA content using Quant-iT Picogreen dsDNA Kit (P7589, Invitrogen, USA). Based on the DNA standard curve of the kit, the content of DNA in the fresh stem samples was compared to the decellularized tubes, and the efficiency was determined by the remanent DNA fraction (in %).

To avoid possible rejection, immunofluorescence analysis for the immunogenic proteins collagen and fibronectin was performed using anti-collagen I, anti-collagen III, and anti-fibronectin (C2456-C7808-GW20021, Sigma, Germany). In the Suppl. Files, additional methodological details are provided for the DNA and SDS quantification, as well as for the biocompatibility analysis.

Quantification of SDS

To examine the residual SDS content in the tubes and indirect potential cytotoxicity, a previously published microliter-volume biochemical analysis was carried out using visible light spectroscopy.[35]

Biocompatibility and proliferative capacity of recellularized celltubes with fibroblasts and endothelial cells

Several circular 3 mm punch biopsy samples were taken from the cell tubes and separately placed in 96 well plates. The control wells were either left without samples or industrial grade dermis replacement (Matriderm) was used. The plates were tested in a microplate reader at a 450 nm and referenced to a wavelength of 620 nm.

As cellulose is biodegradable, implanted tubes must facilitate colonization and inhabitation by patient cell subpopulations, despite small traces of cytotoxic SDS in the implant. Therefore, cell suspensions of isolated fibroblasts from patients and the murine model, as well as commercially obtained HDLECs, were marked with DiO and DiD lipophilic tracers according to the manufacturer's specifications (D3898 -D307, Invitrogen, USA). Using a life imagine device (Azure 600, Biozym, Germany), fluorescence pictures and mean fluorescence signals were obtained at 488 and 644 nm on days 3, 5, and 10 to assess cellular proliferation.

Ex-vivo endothelialization assessment of lymphatic cells in the tubes

For better attachment of cells, the lumen of the tubes was coated with 50 μl poly-D-lysine at a final concentration of 1 mg/ml (7886, Sigma, Germany). The tubes were flushed with 10^4 DiO-stained HDLECs. The tubes were placed horizontally and incubated at 37 °C in a 5% CO_2 atmosphere on

an orbital shaker at 80 rpm for 14 days without additional growth factors.

Tube lymphovenous anastomoses in an *ex-vivo* swine limb model

Previous authors have described the benefits of the porcine in-vivo or *ex-vivo* limb models for supermicrosurgical training of lymphovenous anastomoses.[36-38] Based on these models, we used freshly (< 1 h) harvested posterior swine limbs from a local meat merchant for microsurgical training with the engineered cellulose tubes. A dissecting microscope (F170, Zeiss, Germany), microsurgical instruments (S &T, Neuhausen, Switzerland), and 11-0 monofilament nylon sutures (Ethicon, New Jersey, USA) were used. In accordance with the swine lymphosomes, the lymphatic collectors were identified *ex-vivo* using indocyanine green (ICG) (Verdye, Diagnostic Green, Germany) fluorescence lymphography.

Dehydrated sterile packed cellulose tubes were selected, rehydrated in ringer's solution for 10-15 min, and used as a bypass for an end-to-end anastomosis between a lymphatic collector and a subcutaneous vein. Since the limbs were freshly obtained, a successful patent anastomosis could be tested by injecting fluorescent dye into a downstream skin area and subsequent lymphography. The whole procedure was performed by 3 plastic surgery residents and 4 medical students, all with microsurgical training. An anonymized online survey followed.

Statistical analysis

The arithmetic mean, median, and standard deviation (SD) were calculated and grouped into datasets. All datasets were tested for normal distribution using the Shapiro-Wilk omnibus normality test ($p < 0.05$). For normally distributed datasets one-way ANOVA was applied to determine the overall statistical difference of the paired groups ($p < 0.05$). These results were corrected with Bartlett's test. When the compared groups failed to pass the normality test, a Kruskal-Wallis test with Friedman correction was applied (α 0.05). All the tests were performed using Prism 9.0 (GraphPad, La Jolla, USA). An extensive version of the methods with more details and material description is provided in the Suppl. Files.

Results

Bioengineered cellulose tubes are transparent, variable in size, and storable after dehydration

In this study, 246 cellulose tube were produced, which fulfilled most of the physical characteristics ideally expected from a xenograft for microsurgery. After decellularization, the tubes were nearly completely transparent and presented a sturdy structure and at the same time demonstrated conserved tissue memory and good flexibility necessary for surgical handling (Suppl. Video 1). The size of the tubes generated ranged between 1 mm and 1 cm (average 0.56 mm $\pm$ 0.022), might allow anastomosis of lymphatic collectors as well as small or large blood vessels (Figure 1). These observations were quantified by the kinking resistance test, where the cellulose tube proved to be statistically equally resistant to kinking as decellularized veins, lymphatic collectors, and arteries. Once sterilized using ultraviolet light or gas, the cellulose of the tubes dried completely but remained structurally unchanged and returned to its hydrated flexible form after 10-15 min

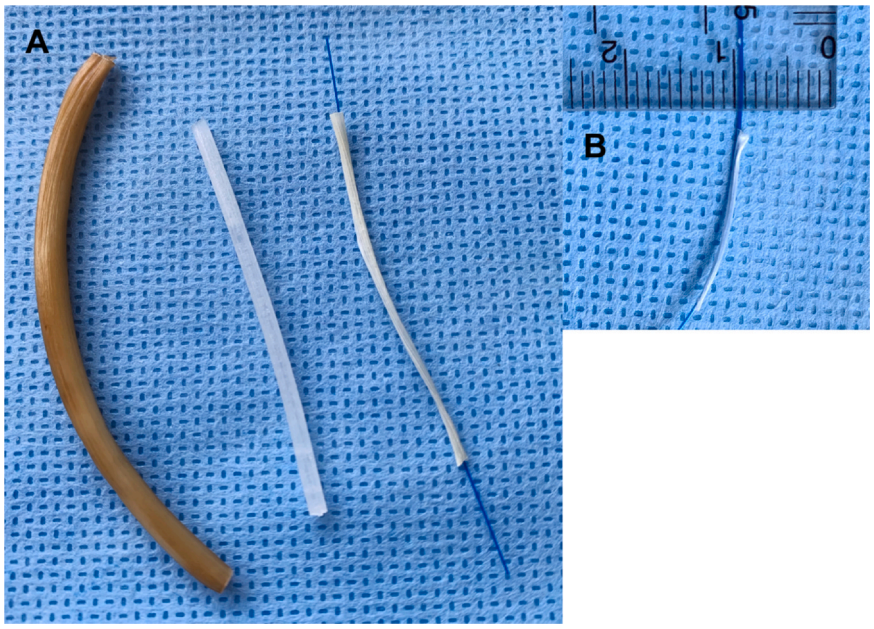

Figure 1 Decellularized cellulose tubes for tissue engineering in lymphatic microsurgery. In **A**, from left to right, the fresh plant stem, decellularized hydrated cellulose tube, and sterilized dehydrated form of the cellulose tube are shown. In **B**, an exemplary demonstration of a 0.4 mm diameter tube for lymphatic supermicrosurgery is provided.

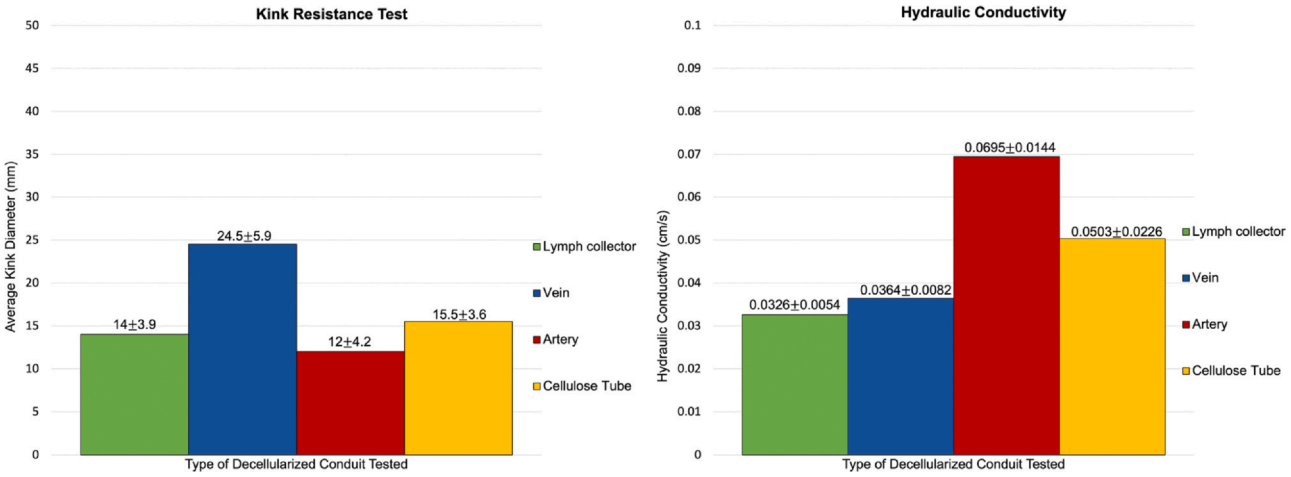

Figure 2 Kinking resistance and hydraulic conductivity results of the engineered cellulose tubes in contrast to decellularized conduits of mammal origin. On the left side, the results of the kink resistance of the conduits are presented. Here, the results best kink resistance (smallest diameter) was found for the decellularized arteries. Also, the best hydraulic conductivity, shown in the right graphic, was found in the swine arteries. The cellulose tube performed at least similarly to decellularized lymph vessels for the kink test and hydraulic conductivity and better than decellularized veins. No statistical significance was found with $p < 0.05$ between any of the groups tested.

incubation in sterile saline (Figure 1). This feature permitted dry and sterile storage for months.

Supplementary material related to this article can be found online at doi:10.1016/j.bjps.2024.05.043.

Cellulose tubes proved to be capillary impermeable and kinking-resistant conduits

Despite being rehydratable, the cellulose tubes proved to be impermeable in low and high capillary pressure output settings (Suppl. Video 2). The hydraulic conductivity in the physiologic range of a lymphangion (65 cm H_2O) and fluid of normal lymph viscosity (0.0018 Pa) was found to be statistically equivalent (α 0.05) to the conductivity of decellularized lymphatic and vascular vessels of the swine (Figure 2). All decellularized conduits demonstrated good kinking resistance and hydraulic conductivity *ex-vivo*, yet an overall better performance was found in decellularized arteries followed by the cellulose tubes. Surprisingly, the least kinking-resistant decellularized vessels were lymphatic collectors and veins, which are the gold standard grafts for current microsurgical anastomoses.

Supplementary material related to this article can be found online at doi:10.1016/j.bjps.2024.05.043.

Cellulose tubes exhibit a characteristic structural polarization

The confocal fluorescence of the cellulose tubes provided a structural correlation that explained the observed physical properties. As shown in Figure 3, the tubes displayed a structural polarization of cellulose. On the abluminal side, the

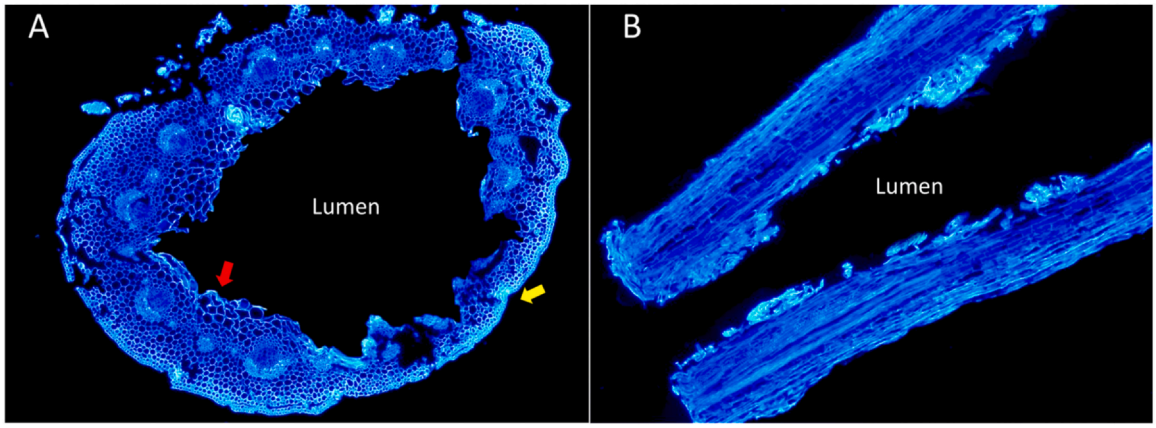

Figure 3 Confocal analysis of the cellulose structure of the bioengineered tube. A cross-sectional and longitudinal view of the tube is demonstrated in **A** and **B,** respectively. The cellulose density is identifiable by the calcofluor white stain, where the signal intensity of cellulose ranges from pale blue to white. The respective polarization of the rather spongiform inner cellulose layer (red arrow) and a dense and compact outer cellulose structure (yellow arrow) provides the tube its mechanical properties.

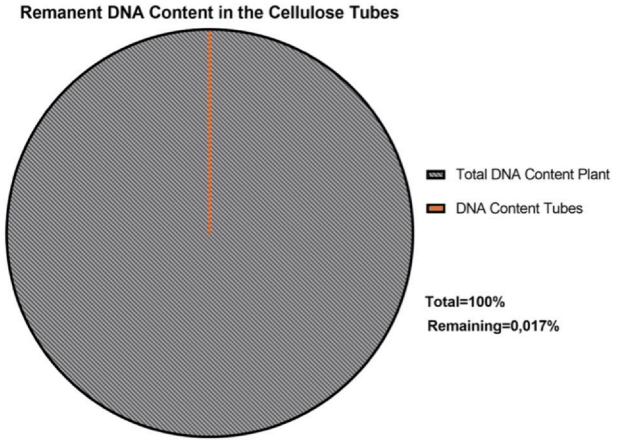

Figure 4 Effectiveness of the decellularization protocol by assessing the residual DNA in the cellulose conduits. The pie chart demonstrates the effectiveness of the applied decellularization protocol in the plant stems, where despite the low doses of SDS used, only 0.017% of the DNA content is detectable. The remaining DNA is 26 times lower than the suggested benchmark for decellularized scaffolds.

cellulose was spongiform with pores that would permit the attachment and infiltration of eukaryotic cells (50 μm) and subsequent endothelization. The external structural pole of the tubes is formed by compact and gapless robust cellulose fibers that might account for structural strength, kink resistance, and impermeability. The polarity of the spongiform cellulose structure on the lumen and strong and compact cellulose exoprotection is a good explanation of the sturdiness of the tubes, which were simultaneously flexible and resistant to deformation (intrinsic tissue memory).

High immunotolerance and low inflammation levels characterize the cellulose tubes

As foreign DNA causes proinflammatory responses and can carry infectious diseases, decellularized xenograft tissue must have almost no residual DNA. The decellularized cellulose tissue used for the tubes had an average of 1.91 ng/mg of dsDNA per mg of dry tissue. This value is less than 0.2% of the total dry tissue weight. Compared to the DNA content of the fresh plant stem, the remaining DNA of the bioengineered tubes was 0.017% (Figure 4). As the recommended benchmark is to obtain < 50 ng of dsDNA per mg of dry tissue in xenografts, our tubes beat the benchmark by 26-fold. In the indirect fluorescence analysis, no nuclear material, collagen, or fibronectin could be detected, which suggests a high immunotolerance potential.

Cellulose tubes have almost no residual cytotoxic SDS and evidenced equivalent biocompatibility in-vitro as Matriderm®

The residual cytotoxic SDS content, determined using photometry, was < 0.1% in all other decellularized conduits tested. The highest remaining SDS concentration was found in decellularized swine arteries with 0.083 ± 0.054% and the lowest was in the cellulose tubes with barely 0.021 ± 0.039% (Figure 5). However, no statistical difference could be found among the groups.

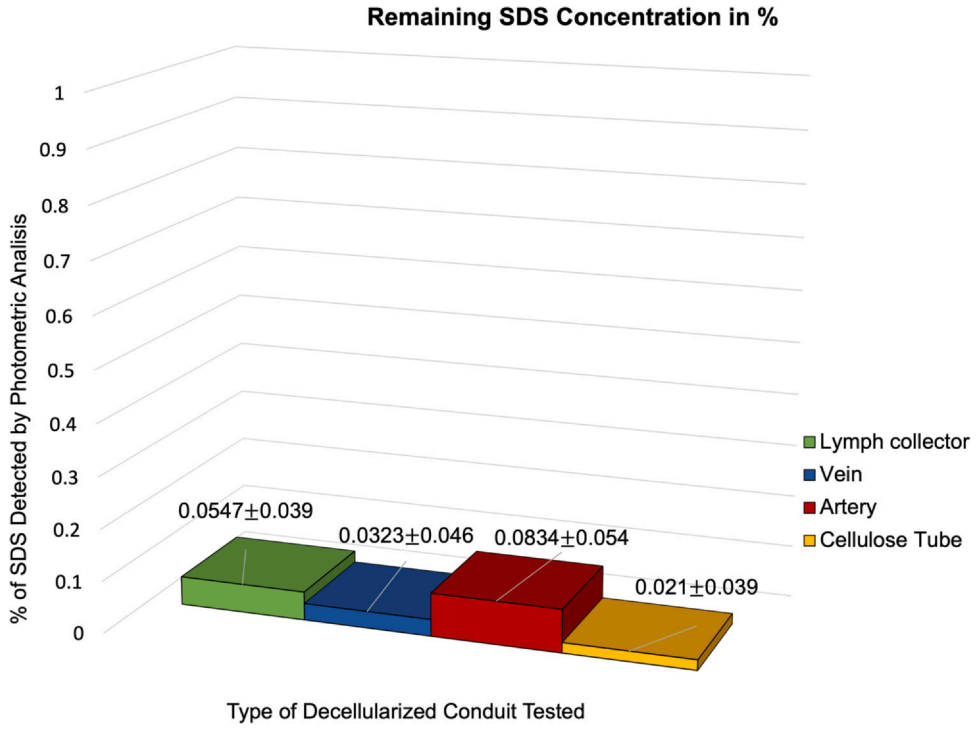

Figure 5 Residual SDS concentration in the decellularized swine vessels and cellulose tubes. In all the conduits decellularized with the protocol described above, low remaining levels of SDS were determined using photometry. All of them presented an SDS concentration < 0.1%, but the cellulose tubes had the lowest concentration of this cytotoxic substance among all the conduits tested. No statistical significance was found among the groups.

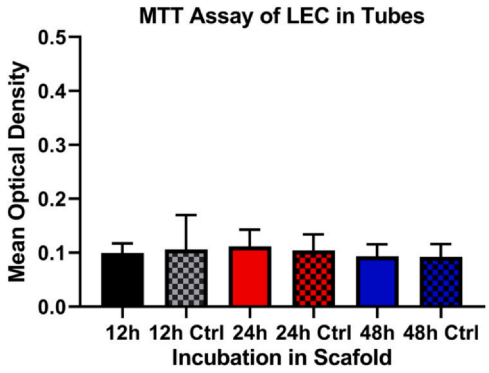

Figure 6 Cytotoxicological analysis of lymphatic endothelial cells within cellulose conduits in contrast to Matriderm®. For different time points, the lymphatic endothelial cells grew without perceived cytotoxicity at all time points. Compared to commercially available dermal substitutes, no significant differences were observed in the cell survival, suggesting that the cellulose tubes might be as safe for the growth of cells as Matriderm®.

Interestingly, no statistical difference in cell growth was found for human lymphatic endothelial cells in-vitro on equivalent sheets of SDS-decellularized cellulose compared to a commercial neo-dermis (Figure 6).

Spontaneous endothelialization occurs in cellulose tubes without growth factors

Fluorescence analysis at 488 nm showed no auto-fluorescence (unspecific signal) or DiO uptake or staining for the control cell-free cellulose tubes (Figure 7).

In contrast, the fluorescence signal of the endothelial cells increased over time in the cross-sectional and longitudinal cellulose tube, implying a survival and progressive proliferation of seeded lymphatic cells in the cellulose conduit (Figure 7).

The results of the median fluorescence intensity for real-time measurement of labeled lymphatic endothelial cells (LEC's) showed that each time point after the LEC seeding exhibited significantly more fluorescence than the

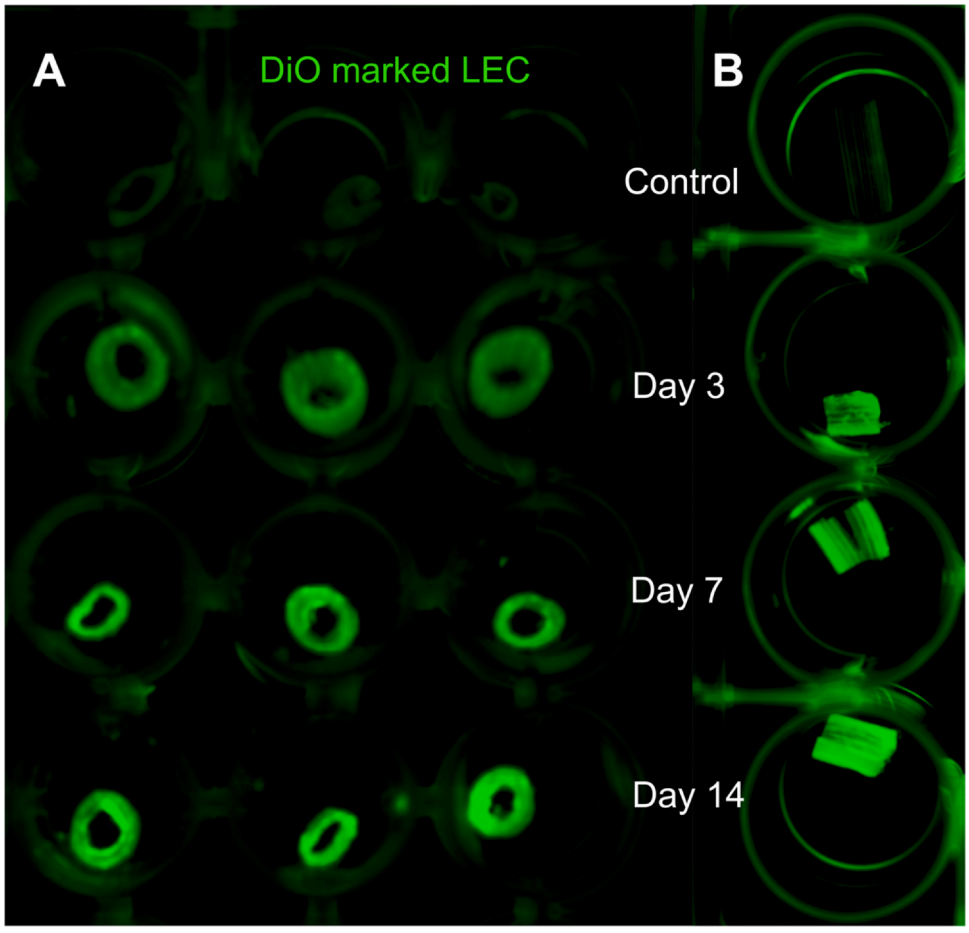

Figure 7 Fluorescence expression of DiO-labeled lymphatic endothelial cells in the cellulose tubes. The cell-free control tubes washed with DiO are presented as a control for DiO-labeled commercially available human endothelial cells grown in-vitro in the bioengineered cellulose tubes. In **A** and **B** the fluorescence signal of the endothelial cells at a wavelength of 488 nm is shown, respectively, for days 3, 7, and 14 of cell culture.

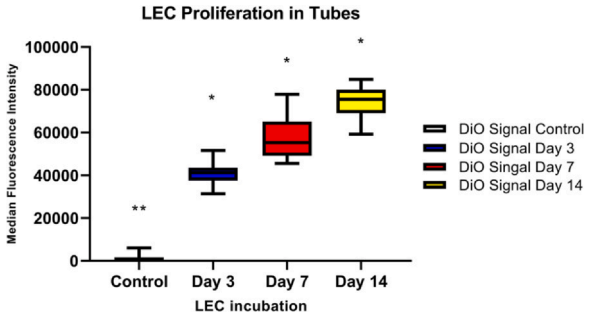

Figure 8 Quantitative evaluation of the mean fluorescence signal of DiO-labeled lymphatic endothelial cells in the cellulose tubes. Real-time fluorescence measurement of labeled LECs in the cellulose tubes was performed in control tubes and on days 3, 7, and 14 (30 per group). The results of the median fluorescence intensity and respective standard deviation are shown in different colors. Statistical significance is shown in the graphic with * for $p < 0.05$ and ** for $p < 0.01$.

preceding time point measured ($p < 0.05$; Figure 8). Each timepoint had significantly higher fluorescence intensity than the control tubes (** for $p < 0.01$), discarding autofluorescence or uptake capability of the tracer by the cellulose conduit (Figure 8).

A close microscopic view at 40X magnification demonstrated the spontaneous infiltration of LEC into the abluminal side of the cellulose tube under culture conditions without added growth factors (Figure 9). Between days 7 and 14, the DiO-labeled LEC's progressively built an endothelial monolayer (day 7) on the inner side of the tube that later progressed to a multilayered lymphatic endothelium (day 14; Figure 9).

Cellulose bioengineered tubes can be used as functional interpositional grafts for lymphovenous anastomosis in an *ex-vivo* swine limb model

The 7 participating surgeons could use the engineered cellulose tubes for 44 lymphatic anastomoses in the swine limb model (Supl. Fig. 1). A total of 72.7% were patent in the ICG lymphography at the first intent, 13.6% after a revision of the anastomosis, and 13.7% never achieved patency (Supl. Fig. 1, C). In the survey, all the surgeons considered the concept, handling, transparency, size, and manipulation resistance to be "good" or "surprisingly good." Nonetheless, all surgeons complained that the cellulose fibers running parallel to the tube, notoriously impeded the anastomosis, as this resulted in recurrent material fatigue that required additional trimming of the tube and re-anastomosis. The main advantage identified by 71% of the surveyed surgeons was the variable size of the cellulose tube permitted to compensate for size mismatches of veins and lymphatics by choosing the appropriate lumen size for each or tailoring it by cutting the tube. With some technical improvements, 100% of the surveyed microsurgeons would consider using bioengineered cellulose tubes for microsurgery, based on this initial experience.

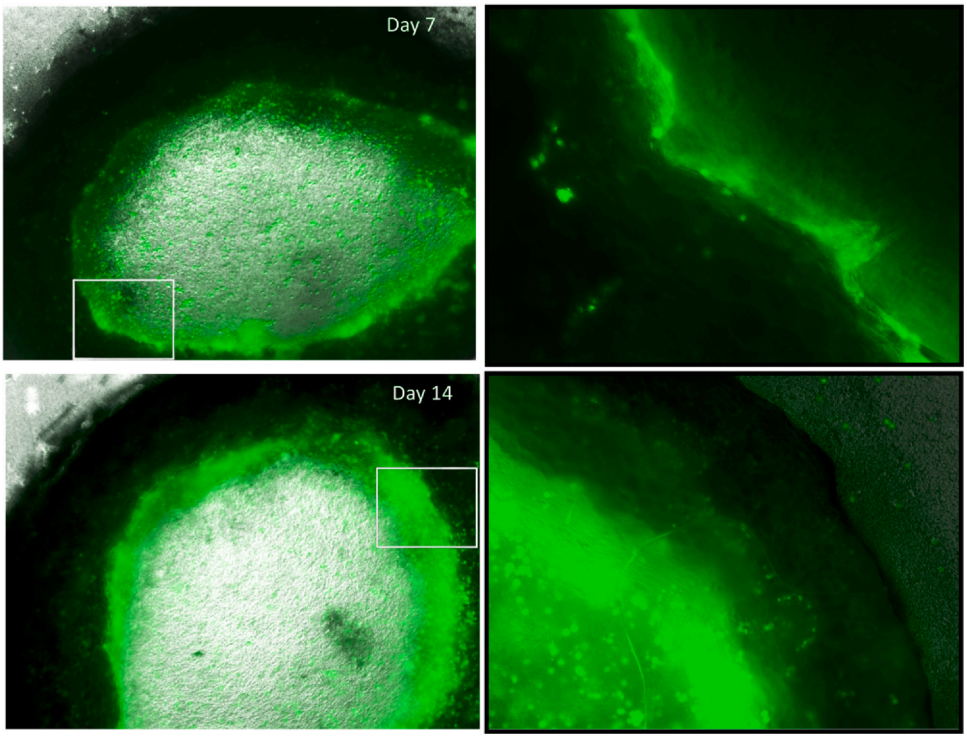

Figure 9 Progressive spontaneous endothelialization of lymphatic endothelial cells in the bioengineered cellulose tubes. Exemplary fluorescence microscopic analysis at a 488 nm wavelength on days 7 (above) and 14 (below) is displayed for DiO-labeled LECs cultivated without growth factors in the cellulose tubes. The images on the right column correspond to a closed up view of the white square of the respective left image.

Discussion

The results presented in this study provide initial evidence of bioengineered cellulose tubes in translational research and microsurgical applications for reconstructive microsurgery, including supermicrosurgery for lymphedema.

Biocompatibility, biodegradability, and abundance make cellulose an attractive material for biomedical purposes.[39,40] Surgical applications are missing despite initial approaches proving its mechanical strength, structural equivalence to mammal extracellular matrix (ECM), and anti-clotting and antimicrobial properties.[41,42] The present study showed that the physical characteristics of the bioengineered cellulose tubes, including transparency, sturdiness, flexibility, and kinking resistance, make them suitable for use as microsurgical interposing grafts. The observed structural polarization of the tubes, with a spongiform structure on the lumen side and robust fibers on the abluminal side, provides resistance to leakage and durability, and enables the attachment and proliferation of cells, thereby facilitating endothelization and tissue integration.

The use of mammal-derived xenograft scaffolds in reconstructive plastic surgery still presents significant challenges. Some ECM proteins found in animal source xenografts, such as alpha-galactosyl epitopes, collagen, and fibronectin can trigger an immune response in humans, leading to graft rejection or inflammation and fibrosis.[43,44] The absence of collagen and fibronectin in the proposed cellulose tubes suggests reduced immunogenicity and the potential for decreased fibrotic responses, making them favorable as microsurgical conduits. Further in-vivo studies are needed to confirm these theoretical benefits and to evaluate the long-term effects of the immune and vascular systems on cellulose interposition grafts.

This is the first evidence that cellulose constructs might have equivalent lymphatic endothelial cells grown as benchmark xenograft material (Matriderm®) without perceived cytotoxicity for all time points in the first 48 h.

Exposure to foreign DNA has raised concerns regarding the potential transmission of infectious agents or activation of the recipient's immune response.[45] Even though decellularization techniques can significantly reduce the DNA content of xenografts,[15] regulators have established strict donor-eligibility criteria and product testing for several viruses, parasites, bacteria, and prions.[46] Such tests substantially increase production costs limiting the use of these products at a global scale.

As no plant is known to be a reservoir of any zoonotic infectious agents, strict scrutiny is not demanded by regulators or ISO standards (ISO 14630:2012) for plant-derived scaffolds.[46] Nevertheless, scientific consensus has defined stringent criteria for complete decellularization and avoidance of proinflammatory responses such as macrophage-related chronic inflammation, fibrosis, or sterile abscess formation.[47] The demand for no visible nuclear material should be found in histological analysis with DAPI or equivalent staining and a total dsDNA of < 50 ng per mg of dry tissue.[48] Our decellularized conduits met the first criteria and, with an average of 1.91 ng/mg, the dsDNA content was 26 times lower than the suggested benchmark.

To prove the utility of the cellulose tube for clinical application, a translational step was required. During this project, a surgical group achieved functional lymphovenous anastomosis by interposing cellulose tube grafts in an *ex-vivo* swine limb model with high ICG-based lymphangiographic patency rates. The surveyed microsurgeons' positive feedback regarding the cellulose tubes for lymphatic microsurgery such as the handling, transparency, size, and ability to compensate for size mismatches in veins and lymphatics, enhanced their versatility as interposition xenografts for reconstructive microsurgery. One technical limitation of our cellulose tubes is that our research laboratory encountered challenges in replicating lymphatic anastomoses at the subcutaneous level with tubes measuring < 0.5 mm in diameter. To address this limitation and the described suture rupture, future tube segments for suturing could be designed with cross-knitted cellulose fibers. Although some anatomic and ultrasonographic studies evidenced average subcutaneous lymphatic vessels of approximately 0.3 mm in healthy distal extremities,[49] other authors have shown that lymphatic collectors in lymphedematous tend to be larger or sclerotic.[10,50,51] In proximal limb segments, the groin, abdomen, or deep collectors lymphatics typically possess larger diameters ranging from 0.8 to 1.2 mm.[52,53] Such collectors or even larger deep lymphatic structures (1.0–3.2 mm) such as the thoracic duct or cisterna chyli,[54] could be reconstructed using the proposed tubes.

Besides its use in lymphatic microsurgery, larger tubes might have clinical potential as vascular interposition grafts for the reconstruction of digital or forearm arteries (0.8–2.8 mm) as interposing graft,[55–57] avoiding unnecessary donor site morbidity and reducing surgical time.[17,58] The proven benefits of cellulose and its conduits in lymphatic microsurgery are in resonance with the modern vascular tissue engineering requirements and further enhance their translational potential.

Others have previously created tubes from bacterial cellulose and even tested such grafts in a murine model. Specifically, Schumann et al. conducted an excellent study in which they demonstrated that tubes made of bacterial cellulose can be implanted in-vivo and support blood flow in pigs for 12 weeks.[59] However, the study had 2 major limitations. As the authors discussed in the article, no biomechanical or in-vivo testing was performed prior to implementation, thus skipping a translational step. Additionally, no data regarding the flow pattern inside the tube were provided, and long-term data regarding the biomechanical stability of the graft after progressive host modification and biodegradation are missing. This is particularly important because bacterial cellulose has not been used as a vascular graft so far, but has mostly been used as filter membranes, wound dressing, and skin substitutes in medicine.[60–62] We preferred plant-based cellulose as vascular grafts because bacterial cellulose fibers have a mere tensile strength of approximately 200 MPa, whereas plant cellulose strength ranges between 750–1080 MPa.[63] Furthermore, bacterial cellulose decomposes faster and is highly dependent on pH and temperature, whereas plant cellulose is less affected by such variables and therefore more reliable in-vivo in the long term.[62,63] The fourfold higher porosity in bacterial cellulose might cause uncontrolled cell migration and fluid leakage into the

interstitium,[63] which is a major concern in lymphedema, where leaky vessels are the primary pathophysiological problem to be address.

In conclusion, we present a novel bioengineered cellulose tube for lymphatic microsurgery aligned with the current research standards for tissue engineering, to fill an existing gap in the field of lymphedema treatment. These demonstrated suitable physical properties, in-vitro spontaneous endothelialization, and successful surgical translation into functional lymphovenous bypasses. Further preclinical investigations are warranted to optimize their design, assess long-term patency, and explore their impact on lymphedema treatment outcomes. In the next translational step, tissue integration, peri-implant host reaction, and long-term capacity to sustain a physiological blood or lymphatic flow should be investigated.

If the cellulose conduits perform as expected in-vivo, several clinical applications might be considered. They could be used following the resection of congenital macrocystic malformations or lymphocele bridging the resulting defect. Moreover, given the limited availability of nearby veins and lymphatics in central lymphatic lesions or complications such as chylothorax or chylous abdomen, interposing grafts could serve as a promising derivative solution to reconstruct the central lymphatic flow.[64] A paradigm change in peripheral secondary lymphedema could be the use of interposing xenografts to bypass lymphosclerotic segments, scars or fibrotic tissue, introducing wider acceptance and better outcomes of LVA in advanced lymphedema stages.[11,65,66] The disparity in size between the lymphatics and the nearby venules has been identified as the primary determinant affecting the appropriate anastomotic configuration and the number of LVAs attained per treated extremity.[67,68] To overcome the size mismatch several salvage techniques were described.[69-71] However, the most effective approach could involve employing tubes of different sizes, each with incremental diameters, as intermediary grafts. This strategy would enable the bypassing of subcutaneous segments until reaching the venule that perfectly matches in size.

These findings pave the way for future innovative approaches in the field of lymphatic microsurgery and lymphatic tissue engineering, holding promise for improving the quality of life for patients with secondary lymphedema.

Funding

None.

Ethical approval

Not required.

Conflicts of interest

Nicole Lindenblatt acts as scientific advisor and consultant for Medical Microinstruments (MMI). All other authors have nothing to disclose.

Appendix A. Supporting information

Supplementary data associated with this article can be found in the online version at doi:10.1016/j.bjps.2024.05.043.

References

1. Ezzo J, Manheimer E, Ml M, et al. Manual lymphatic drainage for lymphedema following breast cancer treatment. *Cochrane Libr* 2015;**2015**:1–4.
2. Lasinski BB, Thrift KM, Squire D, et al. A systematic review of the evidence for complete decongestive therapy in the treatment of lymphedema from 2004 to 2011. *PM R* 2012;**4**:580–601.
3. Scaglioni MF, Fontein DB, Arvanitakis M, Giovanoli P. Systematic review of lymphovenous anastomosis (LVA) for the treatment of lymphedema. *Microsurgery* 2017;**37**:947–53.
4. Basta MN, Gao LL, Wu LC. Operative treatment of peripheral lymphedema: a systematic meta-analysis of the efficacy and safety of lymphovenous microsurgery and tissue transplantation. *Plast Reconstr Surg* 2014;**133**:905–13.
5. Kong X, Du J, Du X, Cong X, Zhao Q. A meta-analysis of 37 studies on the effectiveness of microsurgical techniques for lymphedema. *Ann Vasc Surg* 2022;**86**:440–451.e6.
6. Yamamoto T, Yamamoto N, Yoshimatsu H, Narushima M, Koshima I. Factors associated with lymphosclerosis: an analysis on 962 lymphatic vessels. *Plast Reconstr Surg* 2017;**140**:734–41.
7. Mihara M, Hara H, Hayashi Y, et al. Pathological steps of cancer-related lymphedema: histological changes in the collecting lymphatic vessels after lymphadenectomy. *PLoS One* 2012;**7**:e41126.
8. Gupta N, Verhey EM, Torres-Guzman RA, et al. Outcomes of lymphovenous anastomosis for upper extremity lymphedema: a systematic review. *Plast Reconstr Surg Glob Open* 2021;**9**:e3770.
9. Chun MJ, Saeg F, Meade A, et al. Immediate lymphatic reconstruction for prevention of secondary lymphedema: a meta-analysis. *J Plast Reconstr Aesthet Surg* 2022;**75**:1130–41.
10. Sakai H, Fuse Y, Yamamoto T. Lymphatic vessel diameter and lymphosclerosis: two different characteristics. *Lymphat Res Biol* 2018;**16**:317.
11. Will PA, Hirche C, Berner JE, Kneser U, Gazyakan E. Lymphovenous anastomoses with three-dimensional digital hybrid visualization: improving ergonomics for supermicrosurgery in lymphedema. *Arch Plast Surg* 2021;**48**:427.
12. Yamamoto T, Koshima I. In situ vein grafting for lymphatic supermicrosurgery. *J Plast Reconstr Aesthet Surg* 2014;**67**:e142–3.
13. Koshima I, Inagawa K, Urushibara K, Moriguchi T. Supermicrosurgical lymphaticovenular anastomosis for the treatment of lymphedema in the upper extremities. *J Reconstr Microsurg* 2000;**16**:437–42.
14. Gloviczki P, Hollier LH, Nora FE, Kaye MP. The natural history of microsurgical lymphovenous anastomoses: an experimental study. *J Vasc Surg* 1986;**4**:148–56.
15. Lin CH, Hsia K, Ma H, Lee H, Lu JH. In vivo performance of decellularized vascular grafts: a review article. *Int J Mol Sci* 2018;**19**:495–501.
16. Gui L, Muto A, Chan SA, Breuer CK, Niklason LE. Development of decellularized human umbilical arteries as small-diameter vascular grafts. *Tissue Eng Part A* 2009;**15**:2665–76.
17. Dahl SL, Kypson AP, Lawson JH, et al. Readily available tissue-engineered vascular grafts. *Sci Transl Med* 2011;**3**:68ra9.
18. Li X, Xu J, Bartolák-Suki E, Jiang J, Tien J. Evaluation of 1-mm-diameter endothelialized dense collagen tubes in vascular microsurgery. *J Biomed Mater Res B Appl Biomater* 2020;**108**:2441–9.

19. Chung S, Ingle NP, Montero GA, Kim SH, King MW. Bioresorbable elastomeric vascular tissue engineering scaffolds via melt spinning and electrospinning. *Acta Biomater* 2010;**6**:1958–67.
20. Falkner F, Mayer SA, Thomas B, et al. Acellular human placenta small-diameter vessels as a favorable source of super-microsurgical vascular replacements: a proof of concept. *Bioengineering* 2023;**10**:134–52.
21. Mertens RA, O'Hara PJ, Hertzer NR, Krajewski LP, Beven EG. Surgical management of infrainguinal arterial prosthetic graft infections: review of a thirty-five-year experience. *J Vasc Surg* 1995;**21**:782–90.
22. Jones M, Kujundzic M, John S, Bismarck A. Crab vs. mushroom: a review of crustacean and fungal chitin in wound treatment. *Mar Drugs* 2020;**18**:312–33.
23. Ahmad SI, Ahmad R, Khan MS, et al. Chitin and its derivatives: structural properties and biomedical applications. *Int J Biol Macromol* 2020;**164**:526–39.
24. Varlamov VP, Il'ina AV, Shagdarova BT, Lunkov AP, Mysyakina IS. Chitin/chitosan and its derivatives: fundamental problems and practical approaches. *Biochemistry* 2020;**85**:611–7.
25. Elieh Ali Komi D, Sharma L, Dela Cruz CS. Chitin and its effects on inflammatory and immune responses. *Clin Rev Allergy Immunol* 2018;**54**:213–23.
26. Bamba Y, Ogawa Y, Saito T, Berglund LA, Isogai A. Estimating the strength of single chitin nanofibrils via sonication-induced fragmentation. *Biomacromolecules* 2017;**18**:4405–10.
27. Isobe N, Komamiya T, Kimura S, Kim UJ, Wada M. Cellulose hydrogel with tunable shape and mechanical properties: from rigid cylinder to soft scaffold. *Int J Biol Macromol* 2018;**117**:625–31.
28. Malette W, Quigley H, Adickes E. *Chitosan effect in vascular surgery, tissue culture and tissue regeneration*. Chitin in nature and technology. Springer; 1986. p. 435–42.
29. Ronco C, Clark WR. Haemodialysis membranes. *Nat Rev Nephrol* 2018;**14**:394–410.
30. Binnetoglu A, Demir B, Akakin D, Kervancioglu Demirci E, Batman C. Bacterial cellulose tubes as a nerve conduit for repairing complete facial nerve transection in a rat model. *Eur Arch Otorhinolaryngol* 2020;**277**:277–83.
31. Mandour YM, Mohammed S, Menem MO. Bacterial cellulose graft versus fat graft in closure of tympanic membrane perforation. *Am J Otolaryngol* 2019;**40**:168–72.
32. Spörlein A, Will PA, Kilian K, et al. Lymphatic tissue engineering: a further step for successful lymphedema treatment. *J Reconstr Microsurg* 2021;**37**:465–74.
33. Kanapathy M, Kalaskar D, Mosahebi A, Seifalian AM. Development of a tissue-engineered lymphatic graft using nanocomposite polymer for the treatment of secondary lymphedema. *Artif Organs* 2016;**40**:E1–11.
34. Will PA, Rafiei A, Pretze M, et al. Evidence of stage progression in a novel, validated fluorescence-navigated and microsurgical-assisted secondary lymphedema rodent model. *PLoS One* 2020;**15**:e0235965.
35. Rusconi F, Valton E, Nguyen R, Dufourc E. Quantification of sodium dodecyl sulfate in microliter-volume biochemical samples by visible light spectroscopy. *Anal Biochem* 2001;**295**:31–7.
36. Campisi CC, Jiga LP, Ryan M, et al. Mastering lymphatic microsurgery: a new training model in living tissue. *Ann Plast Surg* 2017;**79**:298–303.
37. Hong JW, Kim YS, Lee WJ, et al. Evaluation of the efficacy of microsurgical practice through time factor added protocol: microsurgical training using nonvital material. *J Craniofac Surg* 2010;**21**:876–81.
38. Suami H, Schaverien MV. Swine hind limb model for super-microsurgical lymphaticovenular anastomosis training. *J Plast Reconstr Aesthet Surg* 2016;**69**:723–5.
39. Kamel R, El-Wakil NA, Dufresne A, Elkasabgy NA. Nanocellulose: from an agricultural waste to a valuable pharmaceutical ingredient. *Int J Biol Macromol* 2020;**163**:1579–90.
40. Dai L, Si C. Recent advances on cellulose-based nano-drug delivery systems: design of prodrugs and nanoparticles. *Curr Med Chem* 2019;**26**:2410–29.
41. Groth T, Wagenknecht W. Anticoagulant potential of regioselective derivatized cellulose. *Biomaterials* 2001;**22**:2719–29.
42. Fan X, Li Y, Li N, et al. Rapid hemostatic chitosan/cellulose composite sponge by alkali/urea method for massive haemorrhage. *Int J Biol Macromol* 2020;**164**:2769–78.
43. Tanemura M, Yin D, Chong AS, Galili U. Differential immune responses to alpha-gal epitopes on xenografts and allografts: implications for accommodation in xenotransplantation. *J Clin Invest* 2000;**105**:301–10.
44. Cooper DK, Good AH, Koren E, et al. Identification of alpha-galactosyl and other carbohydrate epitopes that are bound by human anti-pig antibodies: relevance to discordant xenografting in man. *Transpl Immunol* 1993;**1**:198–205.
45. Fishman JA. Infection in xenotransplantation: opportunities and challenges. *Curr Opin Organ Transpl* 2019;**24**:527–34.
46. Food and Drug Administration, Guidance for Industry: Eligibility Determination for Donors of Human Cells, Tissues, and Cellular and Tissue-based Products (HCT/Ps), May 2015. http://www.fda.gov/cber/gdlns/tissdonor.htm.
47. Badylak SF, Gilbert TW. Immune response to biologic scaffold materials. *Semin Immunol* 2008;**20**:109–16.
48. Gilbert TW, Freund JM, Badylak SF. Quantification of DNA in biologic scaffold materials. *J Surg Res* 2009;**152**:135–9.
49. Hayashi A, Giacalone G, Yamamoto T, et al. Ultra high-frequency ultrasonographic imaging with 70 MHz scanner for visualization of the lymphatic vessels. *Plast Reconstr Surg Glob Open* 2019;**7**:e2086.
50. Hara H, Mihara M. Change of the lymphatic diameter in different body positions. *Lymphat Res Biol* 2021;**19**:249–55.
51. Yamamoto T, Narushima M, Koshima I. Lymphatic vessel diameter in female pelvic cancer-related lower extremity lymphedematous limbs. *J Surg Oncol* 2018;**117**:1157–63.
52. Tourani SS, Taylor GI, Ashton MW. Scarpa fascia preservation in abdominoplasty: does it preserve the lymphatics? *Plast Reconstr Surg* 2015;**136**:258–62.
53. Tourani SS, Taylor GI, Ashton MW. Anatomy of the superficial lymphatics of the abdominal wall and the upper thigh and its implications in lymphatic microsurgery. *J Plast Reconstr Aesthet Surg* 2013;**66**:1390–5.
54. Moazzam S, O'Hagan LA, Clarke AR, et al. The cisterna chyli: a systematic review of definition, prevalence, and anatomy. *Am J Physiol Heart Circ Physiol* 2022;**323**.
55. Remy H, Locatelli F, Maertens A, et al. Arterial grafts for proper palmar digital artery reconstruction: an anatomical study. *Hand Surg Rehabil* 2021;**40**:69–74.
56. Wahood W, Ghozy S, Al-Abdulghani A, Kallmes DF. Radial artery diameter: a comprehensive systematic review of anatomy. *J Neurointerv Surg* 2022;**14**:1274–8.
57. Tao KZ, Chen EY, Ji RM, Dang RS. Anatomical study on arteries of fasciae in the forearm fasciocutaneous flap. *Clin Anat* 2000;**13**:1–5.
58. Dahl SL, Blum JL, Niklason LE. Bioengineered vascular grafts: can we make them off-the-shelf? *Trends Cardiovasc Med* 2011;**21**:83–9.
59. Schumann DA, Wippermann J, Klemm DO, et al. Artificial vascular implants from bacterial cellulose: preliminary results of small arterial substitutes. *Cellulose* 2009;**16**:877–85.
60. Jankau J, Błażyńska-Spychalska A, Kubiak K, et al. Bacterial cellulose properties fulfilling requirements for a biomaterial of choice in reconstructive surgery and wound healing. *Front Bioeng Biotechnol* 2021;**9**:805053.

61. Hakkarainen T, Koivuniemi R, Kosonen M, et al. Nanofibrillar cellulose wound dressing in skin graft donor site treatment. *J Control Release* 2016;**244**:292–301.
62. Picheth GF, Pirich CL, Sierakowski MR, et al. Bacterial cellulose in biomedical applications: a review. *Int J Biol Macromol* 2017;**104**:97–106.
63. Naomi R, Bt Hj Idrus R, Fauzi MB. Plant- vs. bacterial-derived cellulose for wound healing: a review. *Int J Environ Res Public Health* 2020;**17**:67–76.
64. Weissler JM, Cho EH, Koltz PF, et al. Lymphovenous anastomosis for the treatment of chylothorax in infants: a novel microsurgical approach to a devastating problem. *Plast Reconstr Surg* 2018;**141**:277–92.
65. Will PA, Kilian K, Bieback K, et al. Lymphedema-associated fibroblasts are a TGF-ß1 activated myofibroblast subpopulation related to fibrosis and stage progression in patients and a murine microsurgical model. *Plast Reconstr Surg* 2024.
66. Will PA, Berner JE, Hirche C, et al. Treatment of retracted, postsurgical scars and reduction of locoregional edema using a combined three-dimensional approach of liposuction lipofilling, dissecting cannulas, and suspension sutures. *Eur J Plast Surg* 2023;**46**:1357–67.
67. Tsai PL, Wu SC, Lin WC, et al. Determining factors in relation to lymphovascular characteristics and anastomotic configuration in supermicrosurgical lymphaticovenous anastomosis – a retrospective cohort study. *Int J Surg* 2020;**81**:39–46.
68. Lasso JM, Perez Cano R. Practical solutions for lymphaticovenous anastomosis. *J Reconstr Microsurg* 2013;**29**:1–4.
69. Chung JH, Baek SO, Park HJ, et al. Efficacy and patient satisfaction regarding lymphovenous bypass with sleeve-in anastomosis for extremity lymphedema. *Arch Plast Surg* 2019;**46**:46–56.
70. Yamamoto T, Yamamoto N, Ishiura R. Fusion lymphoplasty for diameter approximation in lymphatic supermicrosurgery using two lymphatic vessels for a larger recipient vein. *J Plast Reconstr Aesthet Surg* 2016;**69**:1306–8.
71. Cha HG, Oh TM, Cho MJ, et al. Changing the paradigm: Lymphovenous anastomosis in advanced stage lower extremity lymphedema. *Plast Reconstr Surg* 2021;**147**:199–207.